Original Research

Inverse Agonist Activity of Angiotensin II Receptor Blocker Is Crucial for Prevention of Aortic Aneurysm Formation in Marfan Syndrome

Short title: Inverse agonism of ARB for Marfan Aortopathy

Hiroki Yagi, MD, PhD; Hiroshi Akazawa, MD, PhD; Qing Liu, MD, PhD; Masahiko Umei, MD, PhD; Hiroshi Kadowaki, MD, PhD; Ryo Matsuoka, MD, PhD; Akito Shindo, MD; Shun Okamura, MD; Akiko Saga-Kamo, MD, PhD; Norifumi Takeda, MD, PhD; Issei Komuro, MD, PhD

From Department of Cardiovascular Medicine (H.Y., H.A., Q.L., M.U., H.K., R.M., A.S., S.O., A.S-K., N.T., I.K.), Graduate School of Medicine, The University of Tokyo, Tokyo, Japan; Marfan Syndrome Center (H.Y., N.T.), The University of Tokyo Hospital, Tokyo, Japan.

Correspondence to:
Hiroshi Akazawa, MD., PhD.
Department of Cardiovascular Medicine,
Graduate School of Medicine, The University of Tokyo,
7-3-1 Hongo, Bunkyo-ku, Tokyo 113-8655, Japan.
TEL: +81-3-5800-9260 FAX: +81-3-5800-9182 E-mail: akazawah-tky@umin.ac.jp
ORCID: 0000-0002-3574-9607

Issei Komuro, MD., PhD.
Department of Cardiovascular Medicine,
Graduate School of Medicine, The University of Tokyo,
7-3-1 Hongo, Bunkyo-ku, Tokyo 113-8655, Japan.
TEL: +81-3-5800-6526 FAX: +81-3-3815-2087 E-mail: komuro-tky@umin.ac.jp
ORCID: 0000-0002-0714-7182

***Word count of Manuscript*: words** 6,655
***Total number of Figures*:** 5

Abstract

Background: Marfan syndrome (MFS), an inherited disorder caused by *FBN1* gene mutations, causes fatal aortic aneurysm. Selective angiotensin II (Ang II) type 1 (AT_1) receptor blockade is a preventive option for patients with MFS aortopathy, and recent clinical studies demonstrated that the inhibitory effect of an AT_1 receptor blocker (ARB) losartan on aortic aneurysm growth is equivalent to that of β-blockers. At present, several ARBs are clinically available, and they have drug-specific differences in pharmacological properties. Especially, inverse agonism of ARBs has potential benefits for cardiovascular protection, but its impact on MFS aortopathy remains poorly understood.

Methods: Candesartan-7H is a candesartan derivative which lacks the carboxyl group critical for inverse agonist activity and works as a neutral antagonist for AT_1 receptor. Candesartan cilexetil (1 mg/kg/day), candesartan-7H (1 mg/kg/day or 20 mg/kg/day), or vehicle was administered to *Fbn1*$^{C1041G/+}$ mice, and aortic aneurysm formation was analyzed using echocardiography, histological staining, and *in situ* MMP assay. Activation of TGF-β signaling and mechanosensitive signaling was studied using western blot and immunohistochemical analysis.

Results: Candesartan cilexetil (1 mg/kg/day) and candesartan-7H (20 mg/kg/day) lowered blood pressures equally in *Fbn1*$^{C1041G/+}$ mice, but that candesartan-7H (1 mg/kg/day) did not. Aortic aneurysmal progression in association with aortic wall thickening, degeneration of elastic fibers, deposition of collagen, MMP activation, and TGF-β signaling activation in *Fbn1*$^{C1041G/+}$ mice was significantly suppressed by treatment with candesartan cilexetil (1 mg/kg/day), but not by candesartan-7H even at 20 mg/kg/day. In addition, candesartan cilexetil, but not candesartan-7H, inhibited up-regulation of mechanical stress–responsive transcriptional factor Egr-1 in ascending aorta of *Fbn1*$^{C1041G/+}$ mice.

Conclusions: Our findings support a crucial role of inverse agonist activity of ARB for prevention of mechanical stress-induced AT_1 receptor activation and aortic aneurysm formation in MFS mice.

Key Words:

ARB, G protein-coupled receptor, inverse agonist, Marfan syndrome, thoracic aortic aneurysm

Introduction

Marfan syndrome (MFS) is an autosomal dominant connective tissue disorder that affects cardiovascular, skeletal, ocular, and pulmonary systems [1]. MFS patients are at risk for sudden death in young adulthood due to the development of thoracic aortic aneurysm (TAA) which can progress to aortic dissection or rupture without prior symptoms [2,3]. Currently, prophylactic aortic root surgery can prolong life expectancy, but there is no sovereign remedy that sufficiently restrains the progression of TAA in MFS patients [4].

MFS is caused by mutations in *FBN1* gene, which encodes fibrillin-1 [5-7]. Fibrillin-1 is a major component of microfibrils within the extracellular matrix (ECM), and also controls the bioavailability of transforming growth factor-β (TGF-β), a potent cytokine that regulates proliferation, differentiation, ECM modeling, and apoptosis [8]. Several studies using mouse models demonstrated that excessive activation of TGF-β and its downstream signaling pathways, as the consequence of altered structure of fibrillin-1, was a likely culprit underlying TAA progression in MFS [9,10]. In addition, treatment with angiotensin II (Ang II) type 1 (AT_1) receptor blockers (ARBs) prevented TAA progression in MFS mice by inhibiting TGF-β signaling [11-13]. According to several clinical studies, ARBs (losartan and irbesartan) reduced the rate of aortic root dilatation in MFS patients compared with placebo [14-16], but losartan showed no significant benefit over the β-blocker atenolol for the prevention of aortic root dilatation [17-20].

The AT_1 receptor is a seven transmembrane spanning G protein-coupled receptor (GPCR), and is activated upon binding to Ang II [21,22]. GPCRs are structurally unstable and show significant constitutive activity in an agonist-independent manner [23,24]. The constitutive activity of wild-type AT_1 receptor can be detected even in the absence of endogenous expression of Ang II [25,26]. We and others reported that the AT_1 receptor can be activated by mechanical stress, independently of Ang II, through a conformational switch of the receptor [25,27-31]. The agonist-independent constitutive activity or activation of AT_1 receptor are relevant to the pathogenesis of cardiovascular remodeling [25,32], and can be inhibited by inverse agonist which stabilizes inactive conformation of the receptor, but not by antagonist which blocks agonist-dependent receptor activation through competing with agonist binding to the receptor [23,33]. Therefore, the inverse agonist activity of ARBs provides clinical advantage to inhibit both Ang II-dependent and -independent receptor activation [34]. The activity of inverse agonism is primarily determined by chemical structure of the drug, and thus is a drug-specific property [26,29,35-38].

It was reported that mechanoresponses of vascular smooth muscle cells in MFS mice were impaired [39]. We hypothesized that mechanical stress-induced activation of AT_1 receptor contributes to aortic aneurysm progression in *Fbn1*$^{C1041G/+}$ mice. The aim of this study is to determine the impact of inverse agonist activity on the efficacy of ARB to prevent aortic aneurysm formation in MFS mice.

Methods

Animal studies

All animal experiments were approved by the Ethics Committee for Animal Experiments of the University of Tokyo (P-14-083 and P-20-040), and adhered strictly to the National Institutes of Health Guide for the Care and Use of Laboratory Animals. Mice were housed in groups of 3–4 animals per cage with a 12 h light-dark cycle at a constant room temperature of 22±1°C with a humidity of 50±15%. The mice were fed a standard chow (CE-2; Clea Japan Inc.) and water *ad libitum* during the experimental period. *Fbn1* $^{C1041G/+}$ mice were obtained from the Jackson Laboratory [40,41], and maintained on a C57BL/6J background. Candesartan cilexetil and candesartan-7H were synthesized by Takeda Pharmaceutical Co., Ltd. Eight-week-old male *Fbn1*$^{C1041G/+}$ mice were treated with candesartan cilexetil (1 mg/kg/day), candesartan-7H (low dose: 1 mg/kg/day, high dose: 20 mg/kg/day), or vehicle in drinking water for 8 weeks [32]. Mice were sacrificed to collect tissue samples under anesthesia by intraperitoneal injection of sodium pentobarbital (50 mg/kg).

Transthoracic echocardiography and blood pressure (BP) measurement

Transthoracic echocardiography was performed on mice anesthetized with 2-3% isoflurane inhalation, using a Vevo 2100 system with a 30-MHz probe (FUJIFILM Visualsonics, Inc.) [42]. For evaluation of aortic diameters, a two-dimensional short-axis view was obtained at the level of aortic root, sinotubular junction (STJ), and ascending aorta at 8 (baseline), 12, and 16 weeks of age. BPs and pulse rates were measured in conscious mice at 16 weeks of age by a tail-cuff method (MK-2000ST NP-NIBP MONITOR; Muromachi Kikai Co., Ltd.) [42].

Western blot analysis

Aortic tissues were harvested, and perivascular adipose tissue was thoroughly removed. The ascending thoracic aortas were crushed by cryo-press, and dissolved in RIPA lysis buffer (50m M Tris-HCl, pH 8.0, 150 mM NaCl, 1% NP-40, 1% SDS, 0.5% Na-deoxycholate, 10 mM Okadaic acid) containing protease inhibitor cocktail (cOmplete ULTRA Tablets Mini EASYpack; Roche Diagnostics). The protein concentration was measured using BCA Protein Assay Kit (Thermo Fisher

Scientific). The lysates were mixed with 5x Laemmli Buffer (50 mM Na_2HPO_4, 50 mM NaH_2PO_4, 2% SDS, 5% 2-mercaptoethanol, 50% glycerol, 0.1% bromophenol blue), boiled at 95°C for 5 min, subjected to SDS–PAGE, and transferred to polyvinylidene difluoride membrane (Merck Millipore). The membranes were blocked with 1% bovine serum albumin (Sigma-Aldrich) or 5% skim milk powder (FUJIFILM Wako Pure Chemical Corporation) in TBST (50 mM Tris-HCl , pH 7.6, 150 mM NaCl, 0.05% Tween 20), and incubated with the following primary antibodies: rabbit monoclonal anti-phosphorylated Smad2 (Ser465/467) antibody (Cell Signaling Technology, #3108), rabbit monoclonal anti-Smad2 antibody (Cell Signaling Technology, #5339), rabbit polyclonal anti-phosphorylated ERK1/2 (Thr202/Tyr204) antibody (Cell Signaling Technology, #9101), rabbit polyclonal anti-ERK1/2 antibody (Cell Signaling Technology, #9102), rabbit monoclonal anti-EGR1 antibody (Cell Signaling Technology, #4154), and rabbit monoclonal anti-GAPDH antibody (Cell Signaling Technology, #2118). The membranes were then incubated with horseradish peroxidase-conjugated anti-mouse (Jackson Immuno Research Laboratories, Inc., #115-035-146) or anti-rabbit IgG antibody (Jackson Immuno Research Laboratories, Inc., # 111-035-003). Immunoreactive signals were detected with ECL Prime Western Blotting Detection Reagent (GE Healthcare Biosciences), and acquired using Lumino Graph I (ATTO Corp.). The integrated density per image area of interest was measured using an NIH Image J software (NIH, Research Branch; http://imagej.nih.gov/ij/).

Histological and immunohistochemical analysis

The ascending aortas were excised, fixed immediately in 10% neutralized formalin (Sakura Finetek Japan Co., Ltd.), and embedded in paraffin. Serial 5 μm sections were stained with hematoxylin-eosin (HE) for morphological analysis, elastica van Gieson (EVG) for detection of elastic fibers, Masson's trichrome for detection of collagen fibers, and Alcian blue for staining proteoglycan. Degeneration of elastic fibers was evaluated by calculating the number of elastic fiber breaks per high power field at 4-5 different representative locations of EVG-stained sections, and the numbers were averaged by 2 observers blinded to the genotype and treatment for each mouse [43].

For immunohistochemical analysis, deparaffinized sections were rehydrated, boiled to retrieve antigens (10 mM citrate buffer, pH 6, for phosphorylated Smad2, ERK1/2), and blocked with 10% goat or rabbit serum in PBS for 60 min and with Avidin/Biotin Blocking Kit (Vector Laboratories, Inc.) for 15 min. The sections were incubated with the following primary antibodies: rabbit monoclonal anti-phosphorylated Smad2 antibody (Ser465/467) (Cell Signaling Technology, #3108), rabbit polyclonal

anti-phosphorylated ERK1/2 antibody (Thr202/Tyr 204) (Cell Signaling Technology, #9101). The Vectastain ABC kit (Vector Laboratories, Inc.) and DAB Peroxidase Substrate Kit (Vector Laboratories, Inc.) were used to detect the primary antibodies. The sections were counterstained with hematoxylin and mounted in Mount-Quick (Daido Sangyo Co., Ltd.).

***In situ* matrix metalloproteinase (MMP) activity assay**

In situ MMP assay was performed on freshly frozen OCT-embedded sections (5 μm) of ascending aortas. Fluorescein-conjugated DQ Gelatin from Pig Skin (50 μg/ml, Thermo Fisher Scientific) in a reaction buffer (0.5 M Tris-HCl, pH 7.6, 1.5 M NaCl, 50 mM $CaCl_2$, 2 mM NaN_3) was applied to the sections, and incubated at 37°C for 24 h. Sections for negative control were incubated in the presence of 5 mM EDTA. The sections were mounted in ProLong Gold Antifade Reagent with DAPI (Thermo Fisher Scientific). An all-in-one fluorescence microscope (BZ-9000; Keyence) was used to detect gelatinase (MMP-2 and MMP-9) activity as green fluorescence.

Statistical analysis

All data are expressed as means ± SEM. For two-group comparisons, a two-tailed Student's *t*-test was used. For multiple comparisons, one-way ANOVA with Tukey's multiple comparisons test was used for group comparisons. Values of $P < 0.05$ were considered statistically significant. All data were statistically analyzed using GraphPad PRISM software version 8.0 (GraphPad Software).

Results

Aneurysm formation in *Fbn1*$^{C1041G/+}$ mice is suppressed by treatment with an inverse agonist, but not antagonist, for AT_1 receptor.

We previously reported that candesartan suppressed mechanical stretch–induced helical movement of AT_1 receptor as an inverse agonist, and thereby inhibited mechanical stress-induced AT_1 receptor activation and pressure overload-induced cardiac hypertrophy even in *angiotensinogen*-null mice [25,27]. The tight binding between the carboxyl group at the benzimidazole ring of candesartan and specific residues of the AT_1 receptor is critical for the potent inverse agonist activity of candesartan to inhibit Ang II-independent receptor activation [27,34,36]. A candesartan derivative (candesartan-7H), lacking the carboxyl group critical for inverse agonist activity, inhibits Ang II-dependent AT_1 receptor activation as a neutral antagonist, but cannot inhibit Ang II-independent constitutive activity of AT_1 receptor or mechanical stress-induced AT_1 receptor activation [27,32,34,36].

We previously reported that treatment with candesartan-7H (high dose: 20

mg/kg/day) suppressed Ang II-induced BP elevation in C57BL/6 male mice, almost equally as treatment with candesartan cilexetil (1 mg/kg/day) did [32]. However, treatment with candesartan-7H (low dose: 1 mg/kg/day) had almost no inhibitory effect on Ang II-induced BP elevation [32].

We first treated *Fbn1*$^{C1041G/+}$ mice at 8 weeks of age with vehicle, candesartan cilexetil (1 mg/kg/day), candesartan-7H (1 mg/kg/day), or candesartan-7H (20 mg/kg/day) for 8 weeks. Tail-cuff measurements revealed that candesartan cilexetil (1 mg/kg/day) and candesartan-7H (20 mg/kg/day) equally lowered both systolic and diastolic BP in *Fbn1*$^{C1041G/+}$ mice, but that candesartan-7H (1 mg/kg/day) did not show BP-lowering effect (**Figure 1A**). Pulse rate and body weight were comparable among the groups (**Figure 1 A and 1B**).

We next measured the diameters of aortic root, STJ, and ascending aorta at baseline and 8 weeks after treatment. Notably, candesartan cilexetil almost completely prevented progression of aortic dilatation at all levels of aortic root, STJ, and ascending aorta in *Fbn1*$^{C1041G/+}$ mice (**Figure 2**). However, candesartan-7H, even at a high dose (20 mg/kg/day), did not significantly prevent progression of aortic dilatation (**Figure 2**). Histologically, candesartan cilexetil significantly attenuated aortic wall thickening, degeneration of elastic fibers, deposition of collagen, and MMP activation in ascending aorta of *Fbn1*$^{C1041G/+}$ mice, as compared with treatment with vehicle or candesartan-7H (low dose and high dose) (**Figure 3**). These results suggest that inverse agonist activity of candesartan is crucial for inhibition of aneurysm formation in *Fbn1*$^{C1041G/+}$ mice.

Activation of TGF-β signaling in ascending aorta of *Fbn1*$^{C1041G/+}$ mice is suppressed by treatment with an inverse agonist, but not antagonist, for AT_1 receptor.

Recent studies demonstrated that TGF-β signaling not only via the canonical (Smad-dependent) pathway but also via the non-canonical (Smad-independent) pathway was involved in aortic aneurysm formation in *Fbn1*$^{C1041G/+}$ mice [9-12]. Both immunohistochemical analysis and western blot analysis revealed that phosphorylation levels of Smad2 and ERK1/2 in ascending aorta of *Fbn1*$^{C1041G/+}$ mice were significantly attenuated by treatment with candesartan cilexetil, but not by treatment with vehicle or candesartan-7H (low dose and high dose) (**Figure 4**). These results suggest that inverse agonist activity of candesartan is indispensable for inhibition of both canonical and non-canonical TGF-β signaling activation in the ascending aorta of *Fbn1*$^{C1041G/+}$ mice.

Up-regulation of mechanosensitive Egr-1 protein in ascending aorta of *Fbn1*$^{C1041G/+}$

mice is suppressed by treatment with an inverse agonist, but not antagonist, for AT_1 receptor.

We previously demonstrated that mechanosensitive signaling was aberrantly activated in ascending aorta of *Fbn1*$^{C1041G/+}$ mice and MFS patients [42]. The expression levels of early growth response-1 (Egr-1) protein, a mechanical stress–responsive transcriptional factor [44-46] were significantly increased in ascending aorta of *Fbn1*$^{C1041G/+}$ mice, as compared with *Fbn1*$^{+/+}$ mice (**Figure 5**). Interestingly, treatment with candesartan cilexetil suppressed the up-regulation of Egr-1 protein in ascending aorta of *Fbn1*$^{C1041G/+}$ mice, but treatment with vehicle or candesartan-7H (low dose and high dose) did not (**Figure 5**). These results suggest that inverse agonist activity of candesartan is essential for inhibition of aberrant activation of mechanical stress-induced signaling in the ascending aorta of *Fbn1*$^{C1041G/+}$ mice.

Discussion

In this study, we demonstrated that candesartan cilexetil (1 mg/kg/day), but not candesartan-7H even at a higher dose (20 mg/kg/day), prevented aortic root dilatation, in association with histopathological changes, MMP activation, TGF-β signaling activation, and up-regulation of mechanosensitive Egr-1 protein in ascending aorta of *Fbn1*$^{C1041G/+}$ mice. Candesartan cilexetil (1 mg/kg/day) and candesartan-7H (20 mg/kg/day) equally lowered BP in *Fbn1*$^{C1041G/+}$ mice, suggesting that candesartan-7H can inhibit Ang II-dependent AT_1 receptor activation as a neutral antagonist at a higher dose (20 mg/kg/day), as previously described [32]. Candesartan-7H lacks the carboxyl group of candesartan critical for inverse agonist activity, and cannot inhibit mechanical stress-induced AT_1 receptor activation [27,32,34,36]. Therefore, our study highlights inverse agonist activity as a crucial pharmacological property of ARBs to prevent the progression of TAA in *Fbn1*$^{C1041G/+}$ mice.

The role of the AT_1 receptor in the pathogenesis of MFS aortopathy has been extensively investigated using murine MFS models. Indeed, losartan suppressed aortic root dilatation in *Fbn1*$^{C1041G/+}$ mice [11], but the preventive effect of losartan was not fully observed when Ang II type 2 (AT_2) receptor was knocked out [13]. Although administration of antisense oligonucleotide against angiotensinogen attenuated aortic root dilatation in *Fbn1*$^{C1041G/+}$ mice [47], an angiotensin-converting enzyme inhibitor enalapril, which inhibits Ang II formation and blocks both AT_1 and AT_2 receptor signaling, did not sufficiently inhibit aortic root dilatation, despite showing BP-lowering effects similar to those of losartan [13]. This indicates that the beneficial effects of losartan require activation of AT_2 receptor signaling. However, direct stimulation of

AT_2 receptor with an AT_2 receptor agonist Compound 21 was ineffective for prevention of aortic root dilatation in *Fbn1*$^{C1041G/+}$ mice [48]. A previous study also attributed the beneficial effects of losartan to an AT_1 receptor-independent protection of endothelial function [49]. On the other hand, sequential measurement of aortic dimensions revealed that genetic knockout of AT_1 receptor attenuated aortic root dilatation in *Fbn1*$^{C1041G/+}$ mice [47], indicating that AT_1 receptor activation are crucial for the development of MFS aortopathy.

However, it is still an open question how AT_1 receptor is activated in ascending aorta of MFS, because there has been no evidence of local activation of the renin-angiotensin system. A previous study using aortic tissue of MFS patients showed a significant decrease in AT_1 receptor expression and a significant increase in AT_2 receptor expression, with a significant higher Ang II concentration [50]. Importantly, transcriptomic analysis revealed that the components of renin-angiotensin system were not changed in ascending aorta of *Fbn1*$^{C1041G/+}$ mice [47]. AT_1 receptor is expressed in multiple cell types within aortic tissue, including endothelial cells, vascular smooth muscle cells, fibroblasts, and inflammatory cells [21,22]. Cell type-specific knockout of AT_1 receptor revealed the dominant role of endothelial AT_1 receptor in the pathogenesis of MFS aortopathy in mice. Endothelial cell-specific AT_1 receptor knockout modestly suppressed aortic dilatation and increased survival, whereas smooth muscle cell-specific AT_1 receptor knockout did not show apparent changes in TAA pathology in fibrillin-1 hypomorphic mice (*Fbn1*$^{mgR/mgR}$) [51]. Although it is not fully determined which cell type is most responsible for AT_1 receptor-mediated pathogenesis and how AT_1 receptor is activated, one possible mechanism underlying increased AT_1 receptor signaling in MFS aorta is mechanical stress-induced activation of AT_1 receptor in aortic endothelium.

Mechanical stress is an important trigger to promote aortic dilatation in MFS, as evidenced by both *in vitro* and *in vivo* experiments [46]. Traction force microscopy revealed that force-generating capacity of aortic vascular smooth muscle cells of *Fbn1*$^{mg\Delta lpn/+}$ mice was impaired with disorganization of actin stress fiber network and focal adhesions, indicating mechanoresponse impairment in aortic wall of MFS mice [39]. It was also reported that passive mechanical myocardial tension was reduced in *Fbn1*$^{mgR/mgR}$ mice [52]. Importantly, the cardiomyopathy phenotype in *Fbn1*$^{mgR/mgR}$ mice was restored by genetic knockout of AT_1 receptor or treatment with losartan, but not by genetic knockout of angiotensinogen nor treatment with enalapril [52]. In vascular smooth muscle cells differentiated from MFS patient-derived induced pluripotent stem cells, cyclic stretch increased activation of mechanosensitive β_1-integrin and p38

mitogen-activated protein kinase, leading to exacerbation of MFS phenotype and promotion of apoptosis [53]. It is likely that altered structure and function of fibrillin-1 and inadequate extracellular matrix remodeling may change the stiffness of aortic tissue and perturb normal responses to mechanical forces [46], leading to cellular alterations characteristic of MFS aortopathy. Consistently, acute pressure overload by transverse aortic constriction in wild-type mice was sufficient to induce an aortic smooth muscle cell phenotype, similar to that of *Fbn1*$^{C1041G/+}$ mice [54].

Therefore, it is likely that activation of AT_1 receptor signaling in MFS aorta can be most efficiently prevented by ARBs with potent inverse agonist activity, not by AT_1 receptor antagonists nor by angiotensin-converting enzyme inhibitors, because inverse agonist for AT_1 receptor can inhibit Ang II-independent and mechanical stress-induced receptor activation as well as Ang II-dependent receptor activation [34,36]. Given this background, we demonstrated, in this study, that the loss of inverse agonist activity abolished therapeutic efficacy of candesartan to prevent aortic aneurysm formation in *Fbn1*$^{C1041G/+}$ mice. The potency of inverse agonist activity differs among ARBs according to each chemical structure [36]. Most of ARBs share a common biphenyltetrazole ring structure, and the unique side chain structures contribute to specific drug-receptor bindings that determine inverse agonist activity to stabilize the receptor in an inactive conformation [36]. We previously reported that the bindings of the carboxyl group at the benzimidazole ring of candesartan to specific residues of AT_1 receptor are responsible for the potent inverse agonism in inhibiting mechanical stretch-induced activation of AT_1 receptor [27]. Similarly, drug-receptor interactions involving the carboxyl group and hydroxyl group of olmesartan were essential for potent inverse agonism on stretch-induced AT_1 receptor activation [29]. Although the inverse agonism of commercially available ARBs has not been fully determined, valsartan, irbesartan, azilsartan, and EXP3174 (active metabolite of losartan) also reduce the constitutive GTPase stimulating activity of AT_1 mutant receptor, while losartan does not [26,35,38,55,56]. According to a recent study, a subpressor dose of valsartan attenuated aortic dilatation in *Fbn1*$^{C1041G/+}$ mice, to a similar degree as a pressor dose of losartan. Pharmacological properties including inverse agonist activity may contribute to the difference in therapeutic efficacy between valsartan and losartan [57]. From a view point of inverse agonist activity, head-to-head comparisons of ARBs in preclinical studies will provide a clue to understand the drug effect of ARBs on the prevention of aortic aneurysm formation in MFS.

In conclusion, inverse agonist activity of ARB is crucial for prevention of mechanical stress-induced AT_1 receptor activation and aortic aneurysm formation in

MFS mice. Therefore, we suggest that ARBs with potent inverse agonist activity will have superior therapeutic efficacy. A proof-of-concept implementation will achieve pathophysiology-based optimal medication to restrain the progression of TAA and improve the prognosis and quality of life in MFS patients.

Acknowledgments

None

Sources of Funding

This work was supported in part by grants from Japan Society for the Promotion of Science (KAKENHI 18K08097 and 21K08023 to H.A.), the Japan Agency for Medical Research and Development (Practical Research Project for Rare and Intractable Disease 18ek0109178h0003 to N.T., and CREST JP20gm0810013 to I.K.). H.A. has received scholarship research funds from Takeda Pharmaceutical Co., Ltd. and Nippon Boehringer Ingelheim Co., Ltd. I.K. has received grants from the SENSHIN Medical Research Foundation, and scholarship research funds from Idorsia Pharmaceuticals Japan Ltd., Daiichi Sankyo Co., Ltd., Takeda Pharmaceutical Co., Ltd., and Mitsubishi Tanabe Pharma Corporation.

Disclosures

Drs. Akazawa and Komuro have received scholarship research funds from Takeda Pharmaceutical Co., Ltd.

Nonstandard Abbreviations and Acronyms

Ang II, angiotensin II; ARB, angiotensin II type 1 receptor blocker; Asc Ao, ascending aorta; AT_1 receptor, angiotensin II type 1 receptor; BP, blood pressure; ECM, extracellular matrix; Egr-1, early growth response-1; ERK, extracellular signal-regulated kinase; EVG, elastica van Gieson; GPCR, G protein coupled receptor; HE, hematoxylin-eosin; MFS, Marfan syndrome; STJ, sinotubular junction; TAA, thoracic aortic aneurysm; TGF-β, transforming growth factor-β

References

1. Milewicz DM, Braverman AC, De Backer J, Morris SA, Boileau C, Maumenee IH, Jondeau G, Evangelista A, Pyeritz RE, European Reference Network for Rare Multisystemic Vascular Disease HRDWG. Marfan syndrome. *Nat Rev Dis Primers*. 2021;7:64. doi: 10.1038/s41572-021-00298-7

2. Milewicz DM, Ramirez F. Therapies for Thoracic Aortic Aneurysms and Acute Aortic Dissections. *Arterioscler Thromb Vasc Biol*. 2019;39:126-136. doi: 10.1161/ATVBAHA.118.310956

3. Fletcher AJ, Syed MBJ, Aitman TJ, Newby DE, Walker NL. Inherited Thoracic Aortic Disease: New Insights and Translational Targets. *Circulation*. 2020;141:1570-1587. doi: 10.1161/CIRCULATIONAHA.119.043756

4. Lindeman JH, Matsumura JS. Pharmacologic Management of Aneurysms. *Circ Res*. 2019;124:631-646. doi: 10.1161/CIRCRESAHA.118.312439

5. Lee B, Godfrey M, Vitale E, Hori H, Mattei MG, Sarfarazi M, Tsipouras P, Ramirez F, Hollister DW. Linkage of Marfan syndrome and a phenotypically related disorder to two different fibrillin genes. *Nature*. 1991;352:330-334. doi: 10.1038/352330a0

6. Maslen CL, Corson GM, Maddox BK, Glanville RW, Sakai LY. Partial sequence of a candidate gene for the Marfan syndrome. *Nature*. 1991;352:334-337. doi: 10.1038/352334a0

7. Dietz HC, Cutting GR, Pyeritz RE, Maslen CL, Sakai LY, Corson GM, Puffenberger EG, Hamosh A, Nanthakumar EJ, Curristin SM, et al. Marfan syndrome caused by a recurrent de novo missense mutation in the fibrillin gene. *Nature*. 1991;352:337-339. doi: 10.1038/352337a0

8. Isogai Z, Ono RN, Ushiro S, Keene DR, Chen Y, Mazzieri R, Charbonneau NL, Reinhardt DP, Rifkin DB, Sakai LY. Latent transforming growth factor beta-binding protein 1 interacts with fibrillin and is a microfibril-associated protein. *J Biol Chem*. 2003;278:2750-2757. doi: 10.1074/jbc.M209256200

9. Neptune ER, Frischmeyer PA, Arking DE, Myers L, Bunton TE, Gayraud B, Ramirez F, Sakai LY, Dietz HC. Dysregulation of TGF-beta activation contributes to pathogenesis in Marfan syndrome. *Nat Genet*. 2003;33:407-411. doi: 10.1038/ng1116

10. Ng CM, Cheng A, Myers LA, Martinez-Murillo F, Jie C, Bedja D, Gabrielson KL, Hausladen JM, Mecham RP, Judge DP, et al. TGF-beta-dependent

pathogenesis of mitral valve prolapse in a mouse model of Marfan syndrome. *J Clin Invest*. 2004;114:1586-1592. doi: 10.1172/JCI22715

11. Habashi JP, Judge DP, Holm TM, Cohn RD, Loeys BL, Cooper TK, Myers L, Klein EC, Liu G, Calvi C, et al. Losartan, an AT1 antagonist, prevents aortic aneurysm in a mouse model of Marfan syndrome. *Science*. 2006;312:117-121. doi: 10.1126/science.1124287

12. Holm TM, Habashi JP, Doyle JJ, Bedja D, Chen Y, van Erp C, Lindsay ME, Kim D, Schoenhoff F, Cohn RD, et al. Noncanonical TGFbeta signaling contributes to aortic aneurysm progression in Marfan syndrome mice. *Science*. 2011;332:358-361. doi: 10.1126/science.1192149

13. Habashi JP, Doyle JJ, Holm TM, Aziz H, Schoenhoff F, Bedja D, Chen Y, Modiri AN, Judge DP, Dietz HC. Angiotensin II type 2 receptor signaling attenuates aortic aneurysm in mice through ERK antagonism. *Science*. 2011;332:361-365. doi: 10.1126/science.1192152

14. Groenink M, den Hartog AW, Franken R, Radonic T, de Waard V, Timmermans J, Scholte AJ, van den Berg MP, Spijkerboer AM, Marquering HA, et al. Losartan reduces aortic dilatation rate in adults with Marfan syndrome: a randomized controlled trial. *Eur Heart J*. 2013;34:3491-3500. doi: 10.1093/eurheartj/eht334

15. Milleron O, Arnoult F, Ropers J, Aegerter P, Detaint D, Delorme G, Attias D, Tubach F, Dupuis-Girod S, Plauchu H, et al. Marfan Sartan: a randomized, double-blind, placebo-controlled trial. *Eur Heart J*. 2015;36:2160-2166. doi: 10.1093/eurheartj/ehv151

16. Mullen M, Jin XY, Child A, Stuart AG, Dodd M, Aragon-Martin JA, Gaze D, Kiotsekoglou A, Yuan L, Hu J, et al. Irbesartan in Marfan syndrome (AIMS): a double-blind, placebo-controlled randomised trial. *Lancet*. 2020;394:2263-2270. doi: 10.1016/S0140-6736(19)32518-8

17. Lacro RV, Dietz HC, Sleeper LA, Yetman AT, Bradley TJ, Colan SD, Pearson GD, Selamet Tierney ES, Levine JC, Atz AM, et al. Atenolol versus losartan in children and young adults with Marfan's syndrome. *N Engl J Med*. 2014;371:2061-2071. doi: 10.1056/NEJMoa1404731

18. Forteza A, Evangelista A, Sanchez V, Teixido-Tura G, Sanz P, Gutierrez L, Gracia T, Centeno J, Rodriguez-Palomares J, Rufilanchas JJ, et al. Efficacy of losartan vs. atenolol for the prevention of aortic dilation in Marfan syndrome: a randomized clinical trial. *Eur Heart J*. 2016;37:978-985. doi:

10.1093/eurheartj/ehv575

19. Teixido-Tura G, Forteza A, Rodriguez-Palomares J, Gonzalez Mirelis J, Gutierrez L, Sanchez V, Ibanez B, Garcia-Dorado D, Evangelista A. Losartan Versus Atenolol for Prevention of Aortic Dilation in Patients With Marfan Syndrome. *J Am Coll Cardiol*. 2018;72:1613-1618. doi: 10.1016/j.jacc.2018.07.052

20. Pitcher A, Spata E, Emberson J, Davies K, Halls H, Holland L, Wilson K, Reith C, Child AH, Clayton T, et al. Angiotensin receptor blockers and beta blockers in Marfan syndrome: an individual patient data meta-analysis of randomised trials. *Lancet*. 2022;400:822-831. doi: 10.1016/S0140-6736(22)01534-3

21. de Gasparo M, Catt KJ, Inagami T, Wright JW, Unger T. International union of pharmacology. XXIII. The angiotensin II receptors. *Pharmacol Rev*. 2000;52:415-472.

22. Forrester SJ, Booz GW, Sigmund CD, Coffman TM, Kawai T, Rizzo V, Scalia R, Eguchi S. Angiotensin II Signal Transduction: An Update on Mechanisms of Physiology and Pathophysiology. *Physiol Rev*. 2018;98:1627-1738. doi: 10.1152/physrev.00038.2017

23. Milligan G. Constitutive activity and inverse agonists of G protein-coupled receptors: a current perspective. *Mol Pharmacol*. 2003;64:1271-1276. doi: 10.1124/mol.64.6.1271

24. Rosenbaum DM, Rasmussen SG, Kobilka BK. The structure and function of G-protein-coupled receptors. *Nature*. 2009;459:356-363. doi: 10.1038/nature08144

25. Zou Y, Akazawa H, Qin Y, Sano M, Takano H, Minamino T, Makita N, Iwanaga K, Zhu W, Kudoh S, et al. Mechanical stress activates angiotensin II type 1 receptor without the involvement of angiotensin II. *Nat Cell Biol*. 2004;6:499-506. doi: 10.1038/ncb1137. Epub 2004 May 16.

26. Miura S, Fujino M, Hanzawa H, Kiya Y, Imaizumi S, Matsuo Y, Tomita S, Uehara Y, Karnik SS, Yanagisawa H, et al. Molecular mechanism underlying inverse agonist of angiotensin II type 1 receptor. *J Biol Chem*. 2006;281:19288-19295. doi: 10.1074/jbc.M602144200

27. Yasuda N, Miura S, Akazawa H, Tanaka T, Qin Y, Kiya Y, Imaizumi S, Fujino M, Ito K, Zou Y, et al. Conformational switch of angiotensin II type 1 receptor underlying mechanical stress-induced activation. *EMBO Rep*. 2008;9:179-186.

doi: 10.1038/sj.embor.7401157

28. Mederos y Schnitzler M, Storch U, Meibers S, Nurwakagari P, Breit A, Essin K, Gollasch M, Gudermann T. Gq-coupled receptors as mechanosensors mediating myogenic vasoconstriction. *EMBO J*. 2008;27:3092-3103. doi: 10.1038/emboj.2008.233

29. Qin Y, Yasuda N, Akazawa H, Ito K, Kudo Y, Liao CH, Yamamoto R, Miura S, Saku K, Komuro I. Multivalent ligand-receptor interactions elicit inverse agonist activity of AT(1) receptor blockers against stretch-induced AT(1) receptor activation. *Hypertens Res*. 2009;32:875-883. doi: 10.1038/hr.2009.117

30. Rakesh K, Yoo B, Kim IM, Salazar N, Kim KS, Rockman HA. beta-Arrestin-biased agonism of the angiotensin receptor induced by mechanical stress. *Sci Signal*. 2010;3:ra46. doi: 10.1126/scisignal.2000769

31. Cui Y, Kassmann M, Nickel S, Zhang C, Alenina N, Anistan YM, Schleifenbaum J, Bader M, Welsh DG, Huang Y, et al. Myogenic Vasoconstriction Requires Canonical G(q/11) Signaling of the Angiotensin II Type 1 Receptor. *J Am Heart Assoc*. 2022;11:e022070. doi: 10.1161/JAHA.121.022070

32. Yasuda N, Akazawa H, Ito K, Shimizu I, Kudo-Sakamoto Y, Yabumoto C, Yano M, Yamamoto R, Ozasa Y, Minamino T, et al. Agonist-independent constitutive activity of angiotensin II receptor promotes cardiac remodeling in mice. *Hypertension*. 2012;59:627-633. doi: 10.1161/HYPERTENSIONAHA.111.175208

33. Bond RA, Ijzerman AP. Recent developments in constitutive receptor activity and inverse agonism, and their potential for GPCR drug discovery. *Trends Pharmacol Sci*. 2006;27:92-96. doi: 10.1016/j.tips.2005.12.007

34. Akazawa H, Yano M, Yabumoto C, Kudo-Sakamoto Y, Komuro I. Angiotensin II type 1 and type 2 receptor-induced cell signaling. *Curr Pharm Des*. 2013;19:2988-2995. doi: 10.2174/1381612811319170003

35. Miura S, Kiya Y, Kanazawa T, Imaizumi S, Fujino M, Matsuo Y, Karnik SS, Saku K. Differential Bonding Interactions of Inverse Agonists of Angiotensin II Type 1 Receptor in Stabilizing the Inactive State. *Mol Endocrinol*. 2008;22:139-146. doi: 10.1210/me.2007-0312

36. Akazawa H, Yasuda N, Komuro I. Mechanisms and functions of agonist-independent activation in the angiotensin II type 1 receptor. *Mol Cell*

Endocrinol. 2009;302:140-147. doi: 10.1016/j.mce.2008.11.007.

37. Miura S, Kiya Y, Hanzawa H, Nakao N, Fujino M, Imaizumi S, Matsuo Y, Yanagisawa H, Koike H, Komuro I, et al. Small molecules with similar structures exhibit agonist, neutral antagonist or inverse agonist activity toward angiotensin II type 1 receptor. *PloS One*. 2012;7:e37974. doi: 10.1371/journal.pone.0037974

38. Miura S, Okabe A, Matsuo Y, Karnik SS, Saku K. Unique binding behavior of the recently approved angiotensin II receptor blocker azilsartan compared with that of candesartan. *Hypertens Res*. 2013;36:134-139. doi: 10.1038/hr.2012.147

39. Nolasco P, Fernandes CG, Ribeiro-Silva JC, Oliveira PVS, Sacrini M, de Brito IV, De Bessa TC, Pereira LV, Tanaka LY, Alencar A, et al. Impaired vascular smooth muscle cell force-generating capacity and phenotypic deregulation in Marfan Syndrome mice. *Biochim Biophys Acta Mol Basis Dis*. 2020;1866:165587. doi: 10.1016/j.bbadis.2019.165587

40. Judge DP, Biery NJ, Keene DR, Geubtner J, Myers L, Huso DL, Sakai LY, Dietz HC. Evidence for a critical contribution of haploinsufficiency in the complex pathogenesis of Marfan syndrome. *J Clin Invest*. 2004;114:172-181. doi: 10.1172/JCI20641

41. Kisanuki YY, Hammer RE, Miyazaki J, Williams SC, Richardson JA, Yanagisawa M. Tie2-Cre transgenic mice: a new model for endothelial cell-lineage analysis in vivo. *Dev Biol*. 2001;230:230-242. doi: 10.1006/dbio.2000.0106

42. Yagi H, Akazawa H, Liu Q, Yamamoto K, Nawata K, Saga-Kamo A, Umei M, Kadowaki H, Matsuoka R, Shindo A, et al. Endothelial xanthine oxidoreductase-derived ROS promotes aortic aneurysm formation in Marfan syndrome. https://www.biorxiv.org/content/10.1101/2022.01.30.478356v1.

43. Gallo EM, Loch DC, Habashi JP, Calderon JF, Chen Y, Bedja D, van Erp C, Gerber EE, Parker SJ, Sauls K, et al. Angiotensin II-dependent TGF-beta signaling contributes to Loeys-Dietz syndrome vascular pathogenesis. *J Clin Invest*. 2014;124:448-460. doi: 10.1172/JCI69666

44. Khachigian LM, Anderson KR, Halnon NJ, Gimbrone MA, Jr., Resnick N, Collins T. Egr-1 is activated in endothelial cells exposed to fluid shear stress and interacts with a novel shear-stress-response element in the PDGF A-chain promoter. *Arterioscler Thromb Vasc Biol*. 1997;17:2280-2286. doi:

10.1161/01.atv.17.10.2280

45. Morawietz H, Ma YH, Vives F, Wilson E, Sukhatme VP, Holtz J, Ives HE. Rapid induction and translocation of Egr-1 in response to mechanical strain in vascular smooth muscle cells. *Circ Res*. 1999;84:678-687. doi: 10.1161/01.res.84.6.678

46. Yamashiro Y, Yanagisawa H. The molecular mechanism of mechanotransduction in vascular homeostasis and disease. *Clin Sci (Lond)*. 2020;134:2399-2418. doi: 10.1042/CS20190488

47. Chen JZ, Sawada H, Ye D, Katsumata Y, Kukida M, Ohno-Urabe S, Moorleghen JJ, Franklin MK, Howatt DA, Sheppard MB, et al. Deletion of AT1a (Angiotensin II Type 1a) Receptor or Inhibition of Angiotensinogen Synthesis Attenuates Thoracic Aortopathies in Fibrillin1(C1041G/+) Mice. *Arterioscler Thromb Vasc Biol*. 2021;41:2538-2550. doi: 10.1161/ATVBAHA.121.315715

48. Verbrugghe P, Verhoeven J, Clijsters M, Vervoort D, Schepens J, Meuris B, Herijgers P. The Effect of a Nonpeptide Angiotensin II Type 2 Receptor Agonist, Compound 21, on Aortic Aneurysm Growth in a Mouse Model of Marfan Syndrome. *J Cardiovasc Pharmacol*. 2018;71:215-222. doi: 10.1097/FJC.0000000000000560

49. Sellers SL, Milad N, Chan R, Mielnik M, Jermilova U, Huang PL, de Crom R, Hirota JA, Hogg JC, Sandor GG, et al. Inhibition of Marfan Syndrome Aortic Root Dilation by Losartan: Role of Angiotensin II Receptor Type 1-Independent Activation of Endothelial Function. *Am J Pathol*. 2018;188:574-585. doi: 10.1016/j.ajpath.2017.11.006

50. Nagashima H, Sakomura Y, Aoka Y, Uto K, Kameyama K, Ogawa M, Aomi S, Koyanagi H, Ishizuka N, Naruse M, et al. Angiotensin II type 2 receptor mediates vascular smooth muscle cell apoptosis in cystic medial degeneration associated with Marfan's syndrome. *Circulation*. 2001;104:I282-287. doi: 10.1161/hc37t1.094856

51. Galatioto J, Caescu CI, Hansen J, Cook JR, Miramontes I, Iyengar R, Ramirez F. Cell Type-Specific Contributions of the Angiotensin II Type 1a Receptor to Aorta Homeostasis and Aneurysmal Disease-Brief Report. *Arterioscler Thromb Vasc Biol*. 2018;38:588-591. doi: 10.1161/ATVBAHA.117.310609

52. Cook JR, Carta L, Benard L, Chemaly ER, Chiu E, Rao SK, Hampton TG, Yurchenco P, Costa KD, Hajjar RJ, et al. Abnormal muscle mechanosignaling triggers cardiomyopathy in mice with Marfan syndrome. *J Clin Invest*.

2014;124:1329-1339. doi: 10.1172/JCI71059

53. Granata A, Serrano F, Bernard WG, McNamara M, Low L, Sastry P, Sinha S. An iPSC-derived vascular model of Marfan syndrome identifies key mediators of smooth muscle cell death. *Nat Genet*. 2017;49:97-109. doi: 10.1038/ng.3723

54. Pedroza AJ, Shad R, Dalal AR, Yokoyama N, Nakamura K, Hiesinger W, Fischbein MP. Acute Induced Pressure Overload Rapidly Incites Thoracic Aortic Aneurysmal Smooth Muscle Cell Phenotype. *Hypertension*. 2022;79:e86-e89. doi: 10.1161/HYPERTENSIONAHA.121.18640

55. Miura S, Saku K, Karnik SS. Molecular analysis of the structure and function of the angiotensin II type 1 receptor. *Hypertens Res*. 2003;26:937-943. doi: 10.1291/hypres.26.937

56. Fujino M, Miura S, Kiya Y, Tominaga Y, Matsuo Y, Karnik SS, Saku K. A small difference in the molecular structure of angiotensin II receptor blockers induces AT receptor-dependent and -independent beneficial effects. *Hypertens Res*. 2010;33:1044-1052. doi: 10.1038/hr.2010.135

57. Tehrani AY, White Z, Milad N, Esfandiarei M, Seidman MA, Bernatchez P. Blood pressure-independent inhibition of Marfan aortic root widening by the angiotensin II receptor blocker valsartan. *Physiol Rep*. 2021;9:e14877. doi: 10.14814/phy2.14877

Highlights

- Candesartan cilexetil (inverse agonist for angiotensin II receptor) (1 mg/kg/day) and candesartan-7H (candesartan derivative lacking the carboxyl group critical for inverse agonism) (20 mg/kg/day) equally lower blood pressure in *Fbn1*$^{C1041G/+}$ mice.
- Aortic aneurysm formation in *Fbn1*$^{C1041G/+}$ mice is suppressed by treatment with candesartan cilexetil, but not by candesartan-7H.
- Up-regulation of mechanosensitive Egr-1 protein in ascending aorta of *Fbn1*$^{C1041G/+}$ mice is suppressed by treatment with candesartan cilexetil, but not by candesartan-7H.

Figure legends

Figure 1. Blood pressure (BP) lowering effects of candesartan cilexetil and candesartan-7H in *Fbn1*$^{C1041G/+}$ mice

(A) The systolic and diastolic BP, and pulse rate of 16-week-old vehicle-treated *Fbn1*$^{+/+}$ mice (n = 22) and *Fbn1*$^{C1041G/+}$ mice treated with vehicle (n = 8), candesartan cilexetil (Can) (1 mg/kg/day) (n = 11), candesartan-7H (Can-7H) (1 mg/kg/day) (n = 6), or Can-7H (20 mg/kg/day) (n = 8). The data are mean ± SEM. $^{*}P < 0.05$, $^{***}P < 0.001$, ns, not significant, one-way ANOVA with Tukey's multiple comparisons test.

(B) Body weight of 16-week-old vehicle-treated *Fbn1*$^{+/+}$ mice (n = 23) and *Fbn1*$^{C1041G/+}$ mice treated with vehicle (n = 8), Can (1 mg/kg/day) (n = 11), Can-7H (1 mg/kg/day) (n = 6), or Can-7H (20 mg/kg/day) (n = 8). The data are mean ± SEM. One-way ANOVA with Tukey's multiple comparisons test.

Figure 2. Prevention of aneurysm formation in *Fbn1*$^{C1041G/+}$ mice by candesartan cilexetil, but not by candesartan-7H

(A) Representative ultrasound images of ascending aorta in 16-week-old vehicle-treated *Fbn1*$^{+/+}$ mice and *Fbn1*$^{C1041G/+}$ mice treated with vehicle, candesartan cilexetil (Can) (1 mg/kg/day), candesartan-7H (Can-7H) (1 mg/kg/day), or Can-7H (20 mg/kg/day). Arrowheads indicate aortic root. Scale bar, 1 mm.

(B) Ascending aorta diameters at three different levels (Root, aortic root; STJ, sinotubular junction; Asc Ao, ascending aorta) in 16-week-old vehicle-treated *Fbn1*$^{+/+}$ mice (n = 23) and *Fbn1*$^{C1041G/+}$ mice treated with vehicle (n = 8), Can (1 mg/kg/day) (n = 11), Can-7H (1 mg/kg/day) (n = 6), or Can-7H (20 mg/kg/day) (n = 8) (upper panels). Changes of ascending aorta diameters at Root, STJ, and Asc Ao in vehicle-treated *Fbn1*$^{+/+}$ mice (n = 22) and *Fbn1*$^{C1041G/+}$ mice treated with vehicle (n = 5), Can (1 mg/kg/day) (n = 11), Can-7H (1 mg/kg/day) (n = 6), or Can-7H (20 mg/kg/day) (n = 8) after 8 weeks of treatment (lower panels). The data are mean ± SEM. $^{**}P < 0.01$, $^{***}P < 0.001$, ns, not significant, one-way ANOVA with Tukey's multiple comparisons test.

Figure 3. Prevention of histopathological changes in ascending aorta of *Fbn1*$^{C1041G/+}$ mice by candesartan cilexetil, but not by candesartan-7H

(A) Histological analysis with hematoxylin-eosin (HE) staining, elastica van Geison (EVG) staining, Masson's trichrome staining, and Alcian blue staining in ascending aorta of 16-week-old vehicle-treated *Fbn1*$^{+/+}$ mice and *Fbn1*$^{C1041G/+}$ mice treated

with vehicle, candesartan cilexetil (Can) (1 mg/kg/day), candesartan-7H (Can-7H) (1 mg/kg/day), or Can-7H (20 mg/kg/day). Scale bar, 100 µm.

(B) Measurement of aortic wall thickness and aortic architecture indicated by the number of breaks of the elastic fiber per field in 16-week-old vehicle-treated *Fbn1*$^{+/+}$ mice (n =8) and *Fbn1*$^{C1041G/+}$ mice treated with vehicle (n = 6), Can (1 mg/kg/day) (n = 3), Can-7H (1 mg/kg/day) (n = 4), or Can-7H (20 mg/kg/day) (n = 6). The data are mean ± SEM. $*P < 0.05$, $**P < 0.01$, $***P < 0.001$, one-way ANOVA with Tukey's multiple comparisons test.

(C) *In situ* zymography for gelatinase activity in ascending aorta of 16-week-old vehicle-treated *Fbn1*$^{+/+}$ mice and *Fbn1*$^{C1041G/+}$ mice treated with vehicle, Can (1 mg/kg/day), Can-7H (1 mg/kg/day), or Can-7H (20 mg/kg/day). Scale bars, 100 µm.

Figure 4. Prevention of TGF-β signaling activation in ascending aorta of *Fbn1*$^{C1041G/+}$ mice by candesartan cilexetil, but not by candesartan-7H

(A) Immunostaining for phosphorylated Smad2 (p-Smad2) and phosphorylated ERK1/2 (p-ERK1/2) in ascending aorta of 16-week-old vehicle-treated *Fbn1*$^{+/+}$ mice and *Fbn1*$^{C1041G/+}$ mice treated with vehicle, candesartan cilexetil (Can) (1 mg/kg/day), candesartan-7H (Can-7H) (1 mg/kg/day), or Can-7H (20 mg/kg/day). Scale bars, 100 µm.

(B) Immunoblot analysis of p-Smad2, Smad2, p-ERK1/2, ERK1/2 in ascending aorta of 16-week-old vehicle-treated *Fbn1*$^{+/+}$ mice and *Fbn1*$^{C1041G/+}$ mice treated with vehicle, Can (1 mg/kg/day), Can-7H (1 mg/kg/day), or Can-7H (20 mg/kg/day). The intensity of each band was quantified by densitometric analysis, and quantitation graphs for the p-Smad2/Smad2 (n = 5–9) and p-ERK1/2/ERK1/2 (n = 5–9) are shown (mean ± SEM). $*P < 0.05$, $**P < 0.01$, $***P < 0.001$, one-way ANOVA with Tukey's multiple comparisons test.

Figure 5. Prevention of mechano-sensitive Egr-1 protein up-regulation in ascending aorta of *Fbn1*$^{C1041G/+}$ mice by candesartan cilexetil, but not by candesartan-7H

Immunoblot analysis of Egr-1 protein in ascending aorta of 16-week-old vehicle-treated *Fbn1*$^{+/+}$ mice and *Fbn1*$^{C1041G/+}$ mice treated with vehicle, candesartan cilexetil (Can) (1 mg/kg/day), candesartan-7H (Can-7H) (1 mg/kg/day), or Can-7H (20 mg/kg/day). The intensity of each band was quantified by densitometric analysis and corrected for the amount of Gapdh protein as an internal control (n = 5–9) (mean ± SEM). $*P < 0.05$,

**$P < 0.01$, ***$P < 0.001$, one-way ANOVA with Tukey's multiple comparisons test.

Figure 1.

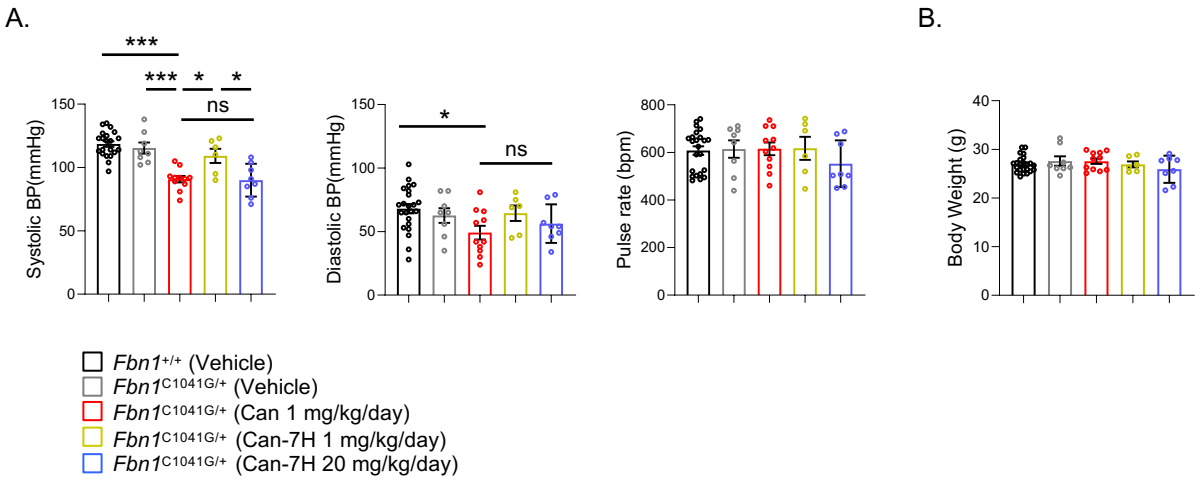
A.
B.
***
***
*
*
ns
*
ns
Systolic BP(mmHg)
Diastolic BP(mmHg)
Pulse rate (bpm)
Body Weight (g)
150
100
50
0
800
600
400
200
40
30
20
10
Fbn1+/+ (Vehicle)
Fbn1C1041G/+ (Vehicle)
Fbn1C1041G/+ (Can 1 mg/kg/day)
Fbn1C1041G/+ (Can-7H 1 mg/kg/day)
Fbn1C1041G/+ (Can-7H 20 mg/kg/day)

Figure 2.

A.

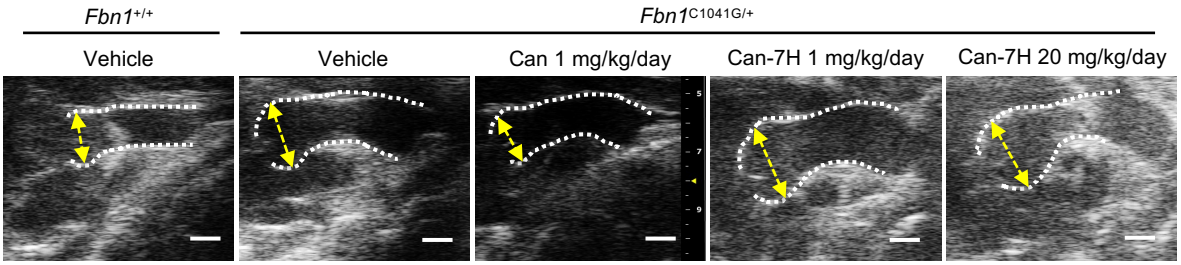

B.

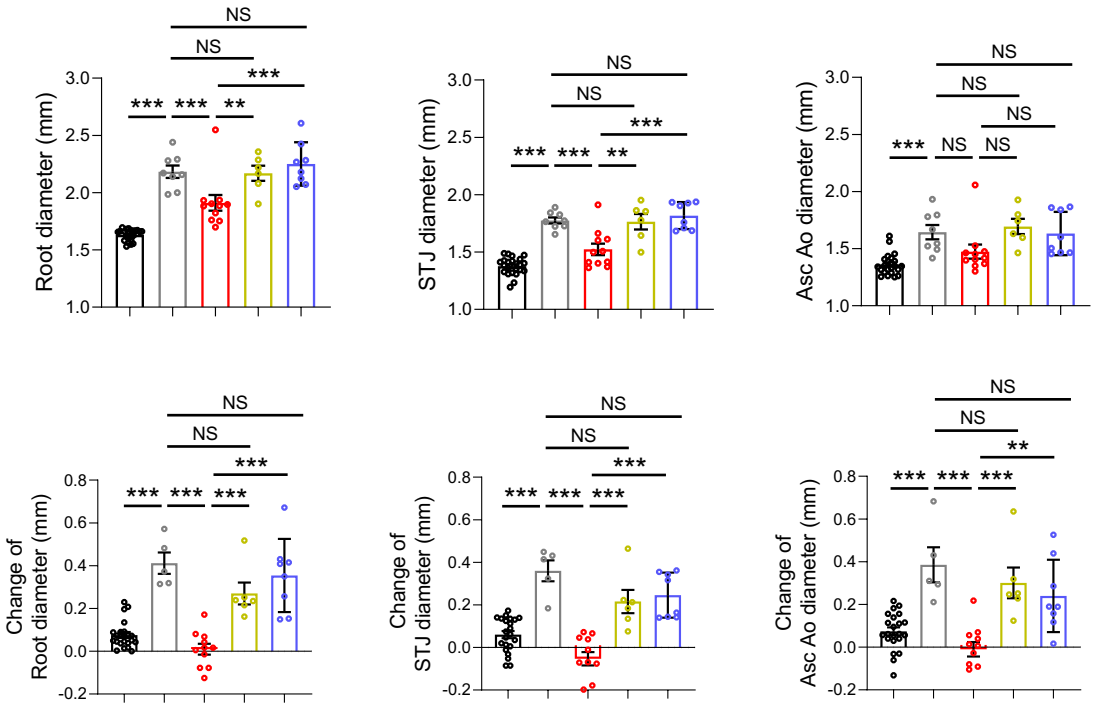

Fbn1+/+ (Vehicle)
Fbn1C1041G/+ (Vehicle)
Fbn1C1041G/+ (Can 1 mg/kg/day)
Fbn1C1041G/+ (Can-7H 1 mg/kg/day)
Fbn1C1041G/+ (Can-7H 20 mg/kg/day)

Figure 3.

A.

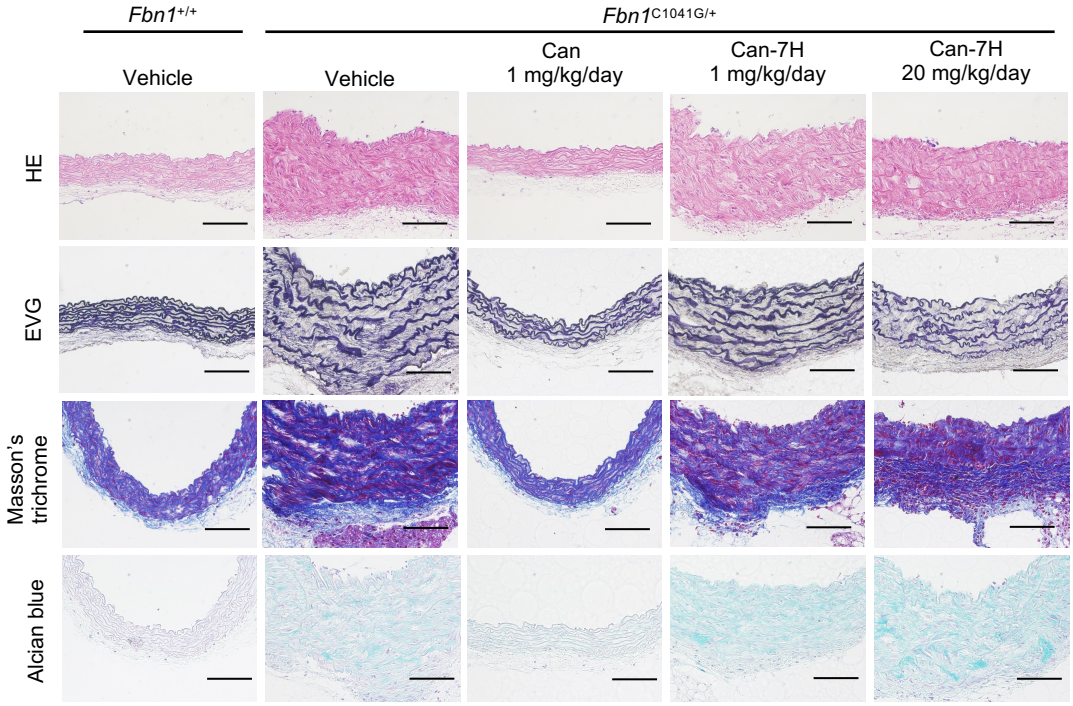
Fbn1+/+
Fbn1C1041G/+
Vehicle
Vehicle
Can
1 mg/kg/day
Can-7H
1 mg/kg/day
Can-7H
20 mg/kg/day
HE
EVG
Masson's trichrome
Alcian blue

B.

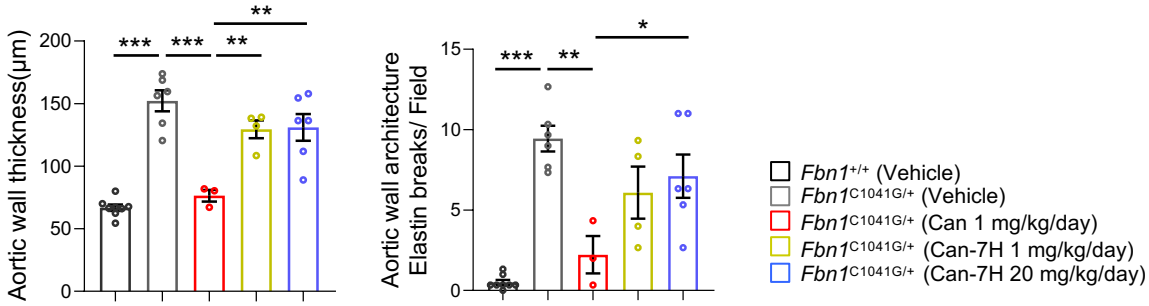
Aortic wall thickness(μm)
200
150
100
50
0
***
***
**
**
Aortic wall architecture
Elastin breaks/ Field
15
10
5
0
***
**
*
Fbn1+/+ (Vehicle)
Fbn1C1041G/+ (Vehicle)
Fbn1C1041G/+ (Can 1 mg/kg/day)
Fbn1C1041G/+ (Can-7H 1 mg/kg/day)
Fbn1C1041G/+ (Can-7H 20 mg/kg/day)

C.

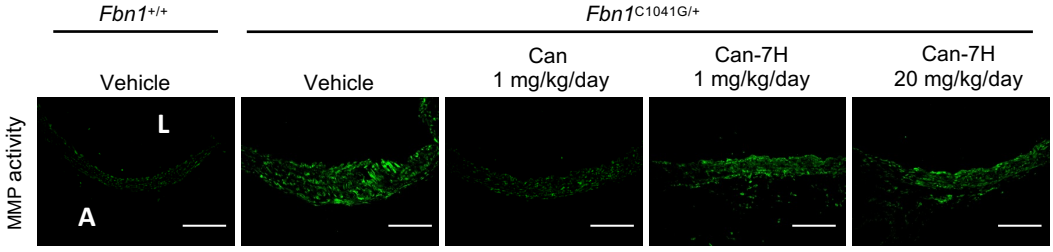
Fbn1+/+
Fbn1C1041G/+
Vehicle
Vehicle
Can
1 mg/kg/day
Can-7H
1 mg/kg/day
Can-7H
20 mg/kg/day
MMP activity
L
A

Figure 4.

A.

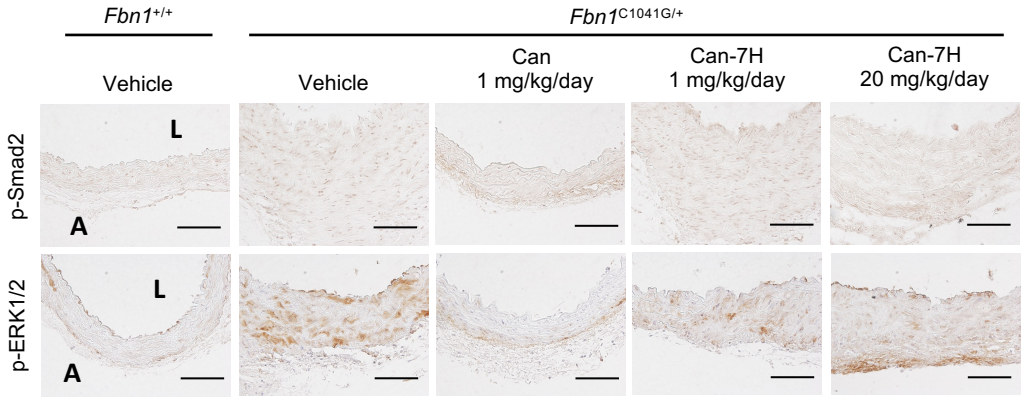
Fbn1+/+
Fbn1C1041G/+
Vehicle
Vehicle
Can
1 mg/kg/day
Can-7H
1 mg/kg/day
Can-7H
20 mg/kg/day
p-Smad2
p-ERK1/2
L
A

B.

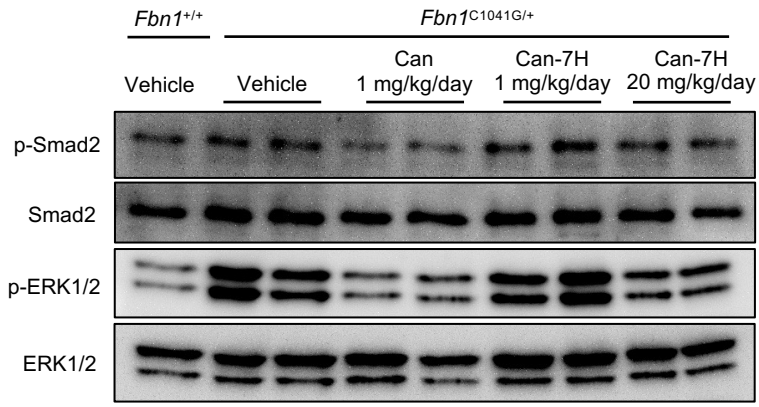
Fbn1+/+
Fbn1C1041G/+
Vehicle
Vehicle
Can
1 mg/kg/day
Can-7H
1 mg/kg/day
Can-7H
20 mg/kg/day
p-Smad2
Smad2
p-ERK1/2
ERK1/2

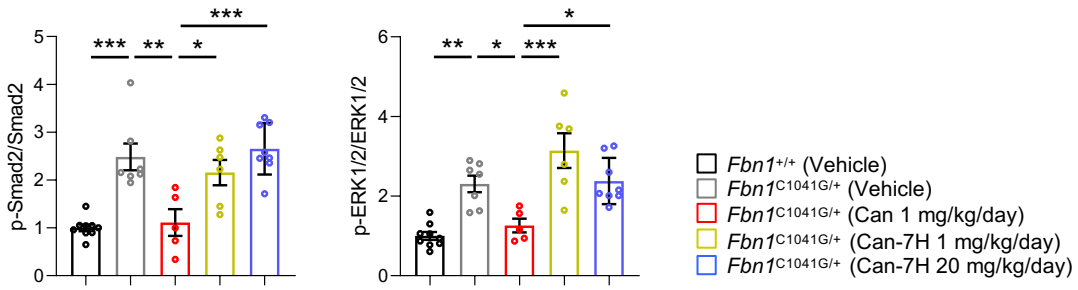
p-Smad2/Smad2
p-ERK1/2/ERK1/2
***
**
*
Fbn1+/+ (Vehicle)
Fbn1C1041G/+ (Vehicle)
Fbn1C1041G/+ (Can 1 mg/kg/day)
Fbn1C1041G/+ (Can-7H 1 mg/kg/day)
Fbn1C1041G/+ (Can-7H 20 mg/kg/day)

Figure 5.

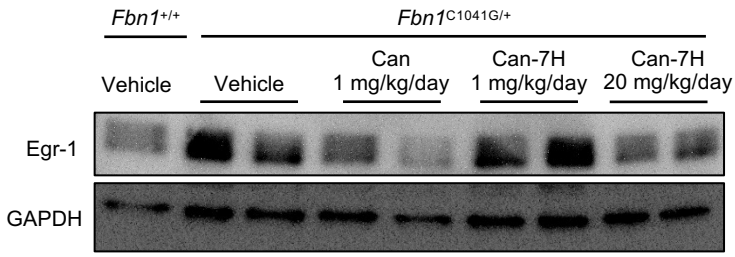
Fbn1+/+
Fbn1C1041G/+
Vehicle
Vehicle
Can
1 mg/kg/day
Can-7H
1 mg/kg/day
Can-7H
20 mg/kg/day
Egr-1
GAPDH

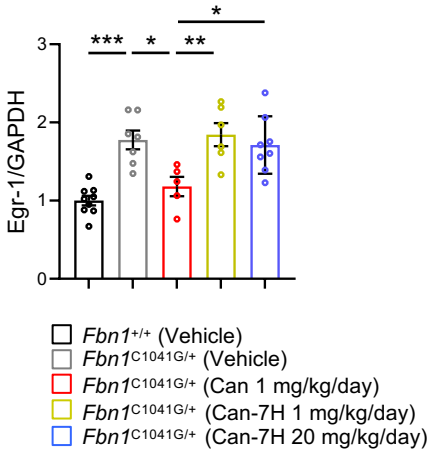
Egr-1/GAPDH
0
1
2
3
***
*
**
*
Fbn1+/+ (Vehicle)
Fbn1C1041G/+ (Vehicle)
Fbn1C1041G/+ (Can 1 mg/kg/day)
Fbn1C1041G/+ (Can-7H 1 mg/kg/day)
Fbn1C1041G/+ (Can-7H 20 mg/kg/day)